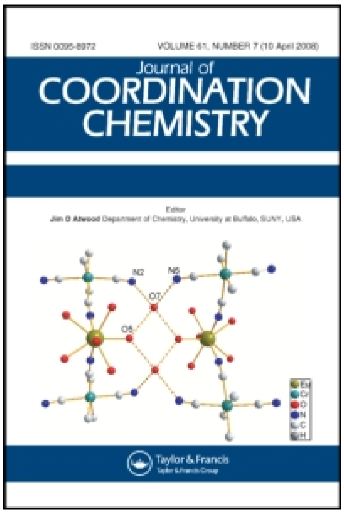

Journal of Coordination Chemistry
Publication details, including instructions for authors and subscription information:
http://www.informaworld.com/smpp/title~content=t713455674

Synthesis, structures, and magnetic properties of a cubane-type cluster $[Ni(hmp)(MeOH)Br]_4 \cdot 2H_2O$ (hmp$^-$= anion of 2-hydroxymethylpyridine)

Fang-Ming Wang[a]; Jian-Guo Lin[a]; Yan-Yan Xing[a]; Yang-Mei Liu[a]; Chang-Sheng Lu[a]; Qing-Jin Meng[a]
[a] State Key Laboratory of Coordination Chemistry, Nanjing National Laboratory of Microstructures, School of Chemistry and Chemical Engineering, Nanjing University, Nanjing 210023, P.R. China

First published on: 31 August 2010

To cite this Article Wang, Fang-Ming , Lin, Jian-Guo , Xing, Yan-Yan , Liu, Yang-Mei , Lu, Chang-Sheng and Meng, Qing-Jin(2010) 'Synthesis, structures, and magnetic properties of a cubane-type cluster $[Ni(hmp)(MeOH)Br]_4 \cdot 2H_2O$ (hmp$^-$= anion of 2-hydroxymethylpyridine)', Journal of Coordination Chemistry, 63: 19, 3431 — 3440, First published on: 31 August 2010 (iFirst)

To link to this Article: DOI: 10.1080/00958972.2010.514048

URL: http://dx.doi.org/10.1080/00958972.2010.514048

Journal of Coordination Chemistry
Vol. 63, No. 19, 10 October 2010, 3431–3440

Taylor & Francis
Taylor & Francis Group

Synthesis, structures, and magnetic properties of a cubane-type cluster $[Ni(hmp)(MeOH)Br]_4 \cdot 2H_2O$ (hmp^- = anion of 2-hydroxymethylpyridine)

FANG-MING WANG*, JIAN-GUO LIN, YAN-YAN XING, YANG-MEI LIU, CHANG-SHENG LU* and QING-JIN MENG

State Key Laboratory of Coordination Chemistry, Nanjing National Laboratory of Microstructures, School of Chemistry and Chemical Engineering, Nanjing University, Nanjing 210023, P.R. China

(*Received 13 April 2010; in final form 13 June 2010*)

$[Ni(hmp)(MeOH)Br]_4 \cdot 2H_2O$ has been prepared by the reaction of 2-hydroxymethylpyridine with $NiBr_2 \cdot 3H_2O$ and characterized by IR, elemental analysis, powder X-ray diffraction, thermogravimetric analyses, magnetic measurements, and single crystal X-ray diffraction. The crystal structure shows two independent $[Ni(hmp)(MeOH)Br]_4$ molecules in the asymmetric unit and $[Ni_4O_4]^{4+}$ cubane-type cores. Each octahedral Ni(II) is bridged by four μ_3-CH_2O^- fragments from four hmp^- ligands. Magnetic studies show that ferromagnetic coupling gives an $S = 4$ ground state with significant magnetoanisotropy, and the parameters are $J_1 = 8.56$, $J_2 = 2.28$, $D = -0.65\,cm^{-1}$, and $g \approx 2.13$.

Keywords: Crystal structure; Cubane nickelate complex; Ferromagnetic coupling; Zero-field splitting

1. Introduction

More than 30 years ago, the field of molecular magnetism came into existence. Chemists used molecules to build up lattices that showed interesting cooperative magnetism, and then designed and prepared solids that exhibited magnetic exchange interactions between the molecular units. Kahn and coworkers [1] reported the first example of a molecular ferrimagnet based on alternating chains of Cu^{II} and Mn^{II} molecular units.

In the early 1990s, chemists discovered the ability of certain molecular transition-metal clusters to be magnetized without the need for long-range cooperative interactions [2–4], first seen in a coordination complex of 12 oxide- and acetate-bridged manganese ions with formula $[Mn_{12}O_{12}(O_2CMe)_{16}(H_2O)_4]$, which was discovered by Friedman *et al.* [5] and Gatteschi and coworkers [6] in 1996 and termed the first

---

*Corresponding authors. Email: wangfmzj@yahoo.com.cn; luchsh@nju.edu.cn

Journal of Coordination Chemistry
ISSN 0095-8972 print/ISSN 1029-0389 online © 2010 Taylor & Francis
DOI: 10.1080/00958972.2010.514048

single-molecule magnets (SMMs). The advent of single-molecule magnetism has stimulated a great deal of research in areas as diverse as physics, theoretical chemistry, spectroscopy, materials chemistry, and synthetic coordination chemistry, as demonstrated by the several hundred papers published on the topic over the past 10 years. For a molecule to be a SMM, it must have three requirements: (1) a high-spin S ground state, (2) appreciable negative magnetoanisotropy, and (3) a weak tunnel splitting that leads to quantum tunneling of the direction of magnetization [7].

Because Ni(II) displays large single-ion anisotropy, many large polynuclear cages of Ni(II) have been studied as a potential route to high-spin molecules [8–12]. Among those compounds, several Ni SMMs have been found [13–16]. Tetranuclear Ni(II) cubanes $[Ni(hmp)(ROH)Cl]_4$ (R = alkyl) with exchange-bias represent a very interesting addition to Ni SMMs [7] with structures and microenvironments that can influence intracluster and intercluster magnetic interactions [17–20].

In order to study the effects of different halides in the clusters, herein, we used $NiBr_2 \cdot 3H_2O$ instead of $NiCl_2 \cdot 2H_2O$ to react with 2-hydroxymethylpyridine and prepared a new tetranuclear Ni(II) cubane-type cluster $[Ni(hmp)(MeOH)Br]_4 \cdot 2H_2O$ (**1**). The crystal structure analysis disclosed that the asymmetric unit of **1** contained two independent $[Ni(hmp)(MeOH)Br]_4$ complexes: one in a general position and the other on an inversion axis. Magnetic studies of **1** showed that there exist stronger intracluster ferromagnetic coupling interactions when bromide, instead of chloride, is coordinated in the clusters.

2. Experimental

2.1. *Chemicals and reagents*

All reagents were purchased from commercial sources and used without purification.

2.2. *Physical measurements*

C, H, and N microanalyses were carried out with a Perkin-Elmer 240 elemental analyzer. The IR spectra were recorded using KBr discs on a Bruker Vector 22 spectrophotometer from 4000 to 400 cm^{-1}. UV-Vis spectra were recorded with a Shimadzu UV-3100 spectrophotometer. Thermogravimetric analyses were performed on a simultaneous SDT 2960 thermal analyzer under flowing N_2 with a heating rate of 10 C min^{-1} between ambient temperature and 700°C. Powder X-ray diffraction (PXRD) was recorded on a Rigaku D/max-RA rotating anode X-ray diffractometer with graphite-monochromatic Cu-Kα ($\lambda = 1.542$ Å) radiation at room temperature. Magnetic susceptibility measurements of polycrystalline samples were measured from 1.8 to 300 K with a Quantum Design MPMS-XL7 SQUID magnetometer under an applied magnetic field of 100–2000 Oe. The field dependences of magnetization were measured using a flux magnetometer in an applied field up to 70 kOe generated by a conventional pulsed technique. Data were corrected for the diamagnetic contribution calculated from Pascal's constants [21].

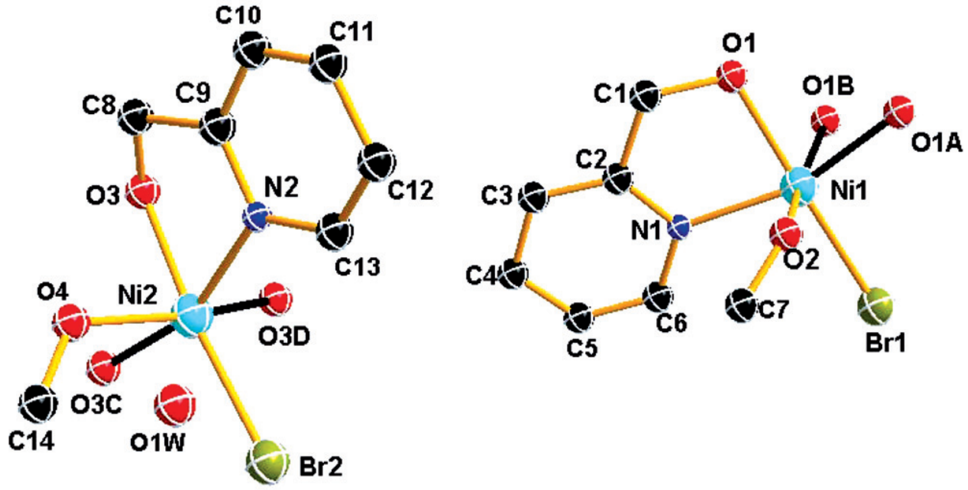

Figure 1. An asymmetric unit representation of **1** (hydrogens omitted for clarity).

2.3. *Synthesis of [Ni(hmp)(MeOH)Br]$_4$•2H$_2$O (1)*

[Ni(hmp)(MeOH)Br]$_4 \cdot 2H_2O$ was synthesized as was [Ni(hmp)(MeOH)Cl]$_4 \cdot H_2O$ [7]. A mixture of $NiBr_2 \cdot 3H_2O$ (2.72 g, 10 mmol), 2-hydroxymethylpyridine (Hhmp) (1.09 g, 10 mmol), and NaOMe (0.54 g, 10 mmol) in 50 mL of MeOH was refluxed for 30 min. The resulting solution was filtered when it was still hot. Green crystals suitable for X-ray analysis were then collected and washed with 10 mL cool MeOH after the solution cooled very slowly; the yield was 24%. Anal. Calcd for $Ni_4C_{28}N_4H_{40}O_{10}Br_4$ (%): C, 29.32; H, 3.51; N, 4.88. Found: C, 29.40; H, 3.36; N, 4.79. Selected IR data (KBr, cm^{-1}): 3384 (br, s), 2904(w), 2840(s), 1607(s), 1571(s), 1481(s), 1441(s), 1363(m), 1287(s), 1220(w), 1153(m), 1072(s), 1048(s), 821(w), 760(s), 729(s), 646(s); UV-Vis (solid, nm): 525, 363, 215.

2.4. *X-ray crystallography*

Crystallographic data for **1** were collected using a Bruker SMART APEX II CCD-based diffractometer with graphite-monochromatic Mo-Kα radiation ($\lambda = 0.71073$ Å) at 291(2) K. Data reductions and absorption corrections were performed with SAINT and SADABS software packages [22], respectively. Structures were solved by direct methods using the SHELXL-97 software package [23]. The non-hydrogen atoms were refined anisotropically using the full-matrix least-squares method on F^2. All hydrogens were placed at calculated positions (C–H = 0.930 Å for benzene, 0.960 Å for methyl and 0.820 Å for –OH) and refined riding on the parent atoms with $U(H) = 1.2U_{eq}$ (bonded C of both pyridyl and methyl group or O atoms) and $U(H) = 1.5U_{eq}$ (bonded C of methyl group). ORTEP drawings of an asymmetric unit and the cubane cluster with labeling scheme of **1** are shown in figures 1 and 2; the crystal packing diagram of the cubane units is shown in figure 3. Details of the crystallographic parameters, data collection, and refinements for **1** are summarized in table 1.

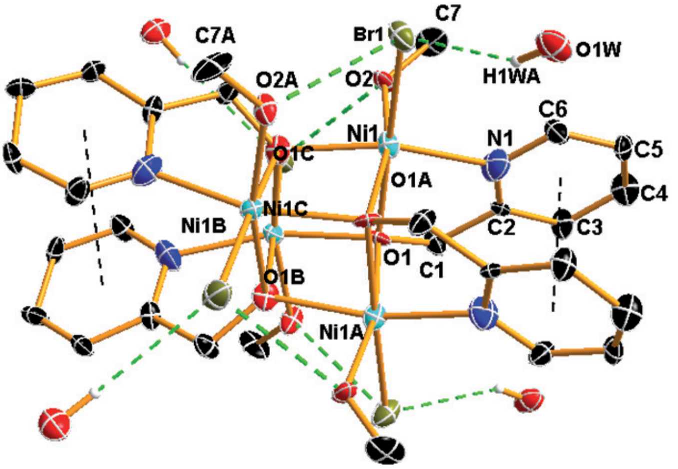

Figure 2. ORTEP representation of cluster showing 30% probability ellipsoids (hydrogens omitted for clarity).

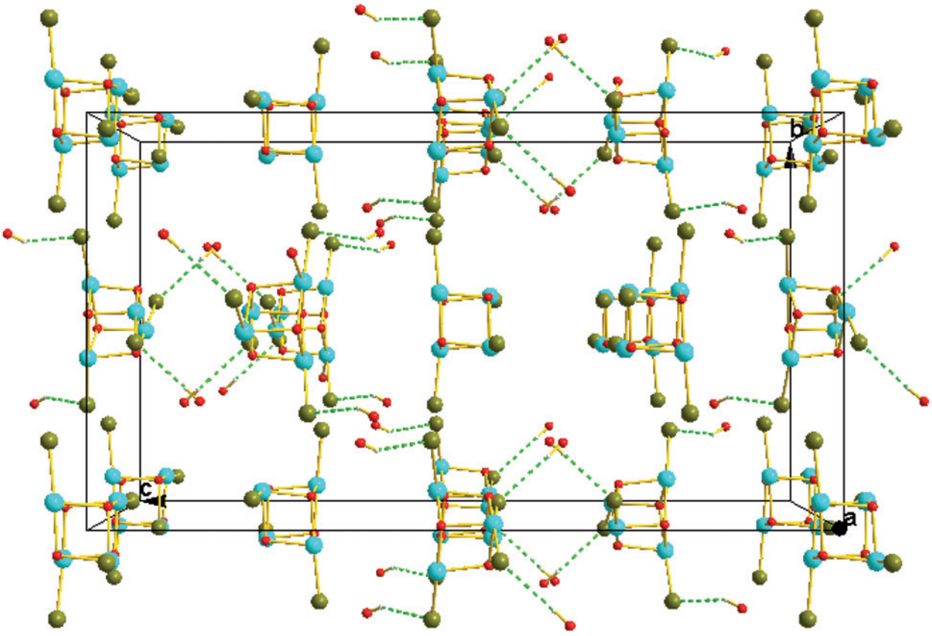

Figure 3. The packing diagram of **1** as viewed along the *a*-axis (H, C, and N omitted for clarity).

3. Results and discussion

3.1. *PXRD and thermal analysis*

The PXRD analysis of **1** closely matches the simulated patterns generated from the results of single-crystal diffraction data (Supplementary material), indicative of pure products.

Table 1. Crystallographic data for **1**.

Empirical formula	$Ni_4C_{28}N_4H_{40}O_{10}Br_4$
Formula weight	1147.00
Temperature (K)	291(2)
Space group	*I*-42*d*
Unit cell dimensions (Å, °)	
a	16.2602(8)
b	16.2602(8)
c	29.548(3)
α	90.00
β	90.00
γ	90.00
Volume (Å^3), Z	7812.3(10), 8
Calculated density (g cm^{-3})	1.950
Absorption coefficient (mm^{-1})	6.045
$F(000)$	4544
Absorption correction	SADABS
Maximum and minimum transmission	0.297 and 0.202
Reflections measured	20,533
Independent reflections	3849 [R(int) = 0.0754]
Reflections observed	3141
Data/restraints/parameters	3849/0/229
Goodness-of-fit on F^2	0.996
R indices [$I > 2\sigma(I)$]^{a,b}	$R = 0.0557$, $R(\omega F^2) = 0.1423$
R indices (all data)^{a,b}	$R = 0.0686$, $R(\omega F^2) = 0.1494$

$^a R_1 = \Sigma||F_o| - |F_c||/\Sigma|F_o|$.
$^b wR_2 = \{\Sigma[w(F_o^2 - F_c^2)^2]/\Sigma[w(F_o^2)^2]\}^{1/2}$.

Thermal decomposition behavior of **1** to 700°C in flowing N_2 (Supplementary material) indicates two mass loss steps below 150°C, corresponding to release of solvated water and coordinated methanol. Mass loss of 1.42% from room temperature to 98°C is from release of half of the solvated water and the second mass loss of 13.37% corresponds to the release of all the coordinated methanol and the other half of the solvated water. The sum of two step experimental mass loss of 14.79% is very close to the calculated value 14.30%. There exists a plateau region ranging from 150°C to 300°C, which supports the fact that the Ni_4 core remains intact after removal of these solution molecules.

3.2. *Description of structure*

The cubane complex **1** crystallizes in the space group *I*-42*d*, where the asymmetric unit contains two independent $[Ni(hmp)(MeOH)Br]_4$ complexes: one in a general position and the other on an inversion axis. In the two different Ni_4 complexes, the differences in the bond distances and angles are relatively small (table 2). Each Ni(II) is chelated by an hmp$^-$ and is also coordinated by bromide, an oxygen from methanol, and two oxygens from two other hmp$^-$ ligands (figure 1). One H_2O solvate is present in the unit also.

As shown in figure 2, there exist two kinds of intramolecular interactions in the cluster. One is O–H $\cdots$ Br hydrogen bond between the OH of methanol and bromide. Although, protons from OH of methanol involved in the hydrogen bond were not

Table 2. Selected bond lengths (Å) and angles (°) for **1**.

Br(1)–Ni(1)	2.3721(14)	C(6)–N(1)–Ni(1)	127.9(6)
Br(2)–Ni(2)	2.3713(15)	C(2)–N(1)–Ni(1)	111.7(6)
N(1)–Ni(1)	2.045(7)	C(13)–N(2)–Ni(2)	127.8(6)
N(2)–Ni(2)	2.100(7)	C(9)–N(2)–Ni(2)	113.3(6)
Ni(1)–O(1A)	2.028(6)	O(1A)–Ni(1)–N(1)	160.8(3)
Ni(1)–O(1)	2.056(6)	O(1A)–Ni(1)–O(1)	81.0(3)
Ni(1)–O(1B)	2.099(6)	N(1)–Ni(1)–O(1)	80.3(3)
Ni(1)–O(2)	2.134(6)	O(1A)–Ni(1)–O(1B)	80.0(3)
Ni(2)–O(3)	2.043(6)	N(1)–Ni(1)–O(1B)	101.5(3)
Ni(2)–O(3C)	2.059(6)	O(1)–Ni(1)–O(1B)	80.5(3)
Ni(2)–O(3D)	2.102(6)	O(1A)–Ni(1)–O(2)	87.1(2)
Ni(2)–O(4)	2.147(7)	N(1)–Ni(1)–O(2)	89.2(3)
O(1)–Ni(1E)	2.028(6)	O(1)–Ni(1)–O(2)	93.0(3)
O(1)–Ni(1B)	2.099(6)	O(1B)–Ni(1)–O(2)	166.3(2)
O(3)–Ni(2F)	2.059(6)	O(1A)–Ni(1)–Br(1)	99.27(17)
O(3)–Ni(2D)	2.102(6)	N(1)–Ni(1)–Br(1)	99.7(2)
O(3)–Ni(2)–N(2)	79.6(3)	O(1)–Ni(1)–Br(1)	174.93(18)
O(3C)–Ni(2)–N(2)	160.5(3)	O(1B)–Ni(1)–Br(1)	94.53(17)
O(3)–Ni(2)–O(3D)	79.2(3)	O(2)–Ni(1)–Br(1)	92.06(18)
O(3C)–Ni(2)–O(3D)	80.6(3)	O(3)–Ni(2)–O(3C)	82.1(2)
N(2)–Ni(2)–O(3D)	102.0(3)	Ni(1E)–O(1)–Ni(1)	99.4(3)
O(3)–Ni(2)–O(4)	91.3(3)	C(1)–O(1)–Ni(1B)	116.3(5)
O(3C)–Ni(2)–O(4)	89.7(2)	Ni(1E)–O(1)–Ni(1B)	98.1(2)
N(2)–Ni(2)–O(4)	84.4(3)	Ni(1)–O(1)–Ni(1B)	98.8(3)
O(3D)–Ni(2)–O(4)	167.3(2)	C(7)–O(2)–Ni(1)	131.1(7)
O(3)–Ni(2)–Br(2)	173.6(2)	C(8)–O(3)–Ni(2)	110.7(5)
O(3C)–Ni(2)–Br(2)	99.89(18)	C(8)–O(3)–Ni(2F)	127.6(6)
N(2)–Ni(2)–Br(2)	99.1(2)	Ni(2)–O(3)–Ni(2F)	98.6(3)
O(3D)–Ni(2)–Br(2)	95.06(16)	C(8)–O(3)–Ni(2D)	118.2(6)
O(4)–Ni(2)–Br(2)	94.80(19)	Ni(2)–O(3)–Ni(2D)	100.6(3)
C(1)–O(1)–Ni(1E)	129.1(6)	Ni(2F)–O(3)–Ni(2D)	96.7(2)
C(1)–O(1)–Ni(1)	110.1(4)	C(14)–O(4)–Ni(2)	129.5(7)

Symmetry transformations used to generate equivalent atoms for **1**: (A) $x+42$, $y+1$, $z-1$; (B) $-x+2$, $-y+1$, z; (C) $-y+1$, x, $-z+1$; (D) $-x+1$, $-y+1$, z; (E) $x+42$, y, $z+1$; (F) y, $-x+1$, $-z+1$.

found from the real F map in **1**, the O $\cdots$ Br distances 2.996(3) and 3.029(3) Å are close to those which indicate the presence of strong hydrogen bonds [7]. The other intramolecular interaction is the $\pi \cdots \pi$ interaction which exists between nearby pyridyl rings of hmp$^-$. The centroid–centroid distances and dihedral angle between pyridyl ring planes are 3.675 Å and 23.5°.

Intermolecular H-bonding interactions between the solvated water and bromide are also observed (with H-bonding parameters of $d_{O \cdots Br} = 3.570(8)$ Å and $\angle$O–H $\cdots$ Br = 154.3°).

3.3. *Magnetic susceptibilities of [Ni(hmp)(MeOH)Br]$_4$ • 2H$_2$O*

Magnetic measurements were performed on polycrystalline samples of **1**. The temperature dependencies of susceptibility under 2 kOe for **1** are displayed in figure 4. At room temperature, the $\chi_M T$ value is 4.95 emu K mol^{-1}. Upon decrease in temperature, $\chi_M T$ values increase slowly and reach 6.10 emu K mol^{-1} at 80 K and then abruptly increase, reaching a maximum value 11.88 emu K mol^{-1} at 9 K, suggesting

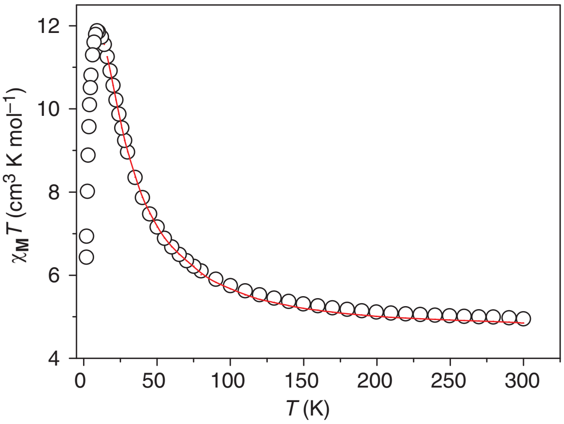

Figure 4. Plots of $\chi_M T$ *vs.* T for **1** at a field of 2 kOe (circles represent experimental data and solid lines the best fitting of the data).

ferromagnetic coupling between Ni^{II} ions. After 9 K, the $\chi_M T$ values decrease to 6.44 emu K mol^{-1} at 1.8 K. This magnetic behavior could be attributed to the presence of significant zero-field splitting in the ground state, weak intermolecular antiferromagnetic interactions, or Zeeman effects [24]. The maximum $\chi_M T$ value of **1** is larger than that of [Ni$_4$(Pym)$_4$Cl$_4$(CH$_3$OH)$_4$] (8.1 emu K mol^{-1}) [25], which means that ferromagnetic coupling interaction in the clusters is enhanced when chloride is changed to bromide.

To account for the cubane complex having S_4 site symmetry, which is lower than T_d, a lower symmetry two-J model was employed to fit the $\chi_M T$ data [18]. The spin Hamiltonian for this case is:

$$\hat{H} = -2J_1(\hat{S}_1 \cdot \hat{S}_2 + \hat{S}_3 \cdot \hat{S}_4) - (-2J_2)(\hat{S}_1 \cdot \hat{S}_3 + \hat{S}_1 \cdot \hat{S}_4 + \hat{S}_2 \cdot \hat{S}_3 + \hat{S}_2 \cdot \hat{S}_4). \quad (1)$$

We used equation (1) and the best fit parameters were found to be $J_1 = 8.56$, $J_2 = 2.28$, and $g = 2.13$. The positive values for J_1 and J_2 mean that ferromagnetic interaction exists in the cluster.

The magnetization was measured in fields up to 70 kOe at a fixed temperature of 1.8 K. As displayed in figure 5, the experimental values of variable-field magnetization are higher than the Brillouin curves corresponding to $S = 4$, suggesting ferromagnetic Ni^{II}–Ni^{II} interaction. The magnetization at saturation per Ni$_4^{II}$ unit is 10.41 $N\beta$ mol^{-1} at 7 T ($S_{Ni} = 1$ and $g_{Ni} = 2.0$), also confirming that intracluster ferromagnetic coupling existing in the cluster.

Temperature dependence data for the magnetization were collected at a variety of fields from 1.8 to 10 K (figure 6a). In the M *versus* H/T plot, a non-superposition of the lines in different magnetic fields is observed, suggesting the existence of zero-field splitting in **1**. With the spin ground state $S = 4$, fits of the magnetization data using ANISOFIT 2.0 [26] for $T \leq 5$ K and $H \geq 1$ T afforded $D = -0.65$ cm^{-1} and $g = 2.14$ (figure 6b). The g and D values are comparable to those of reported Ni$_4^{II}$ clusters [27]. The D values obtained in the reduced-magnetization fitting are averages for two crystallographically independent molecules in the crystal of complex.

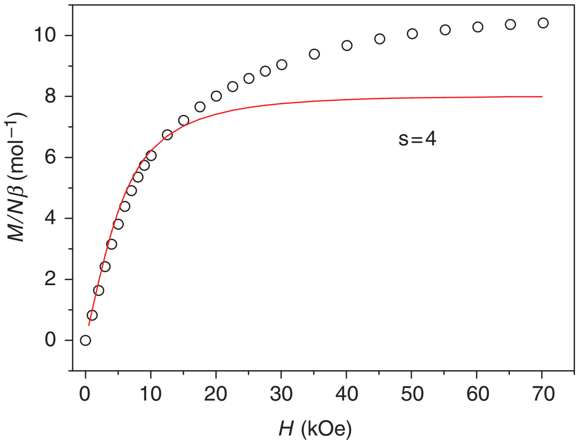

Figure 5. Plots showing magnetization *vs.* field up to $H = 70$ kOe at 1.8 K (circles represent experimental data and solid lines the Brillouin function that corresponds to non-interacting $S = 4$).

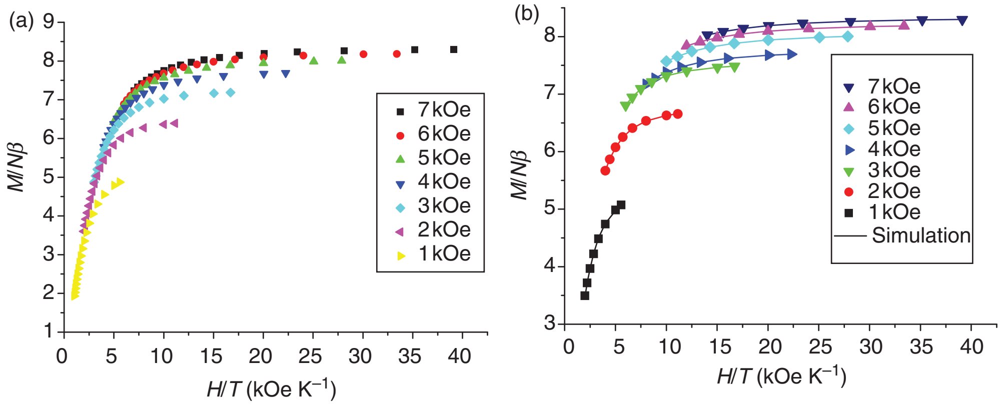

Figure 6. Plots of magnetization *vs.* H/T for **1** between 1.8 and 5.0 K (solid lines represent fits to the data).

4. Conclusions

$[Ni(hmp)(MeOH)Br]_4 \cdot 2H_2O$ was prepared by reaction of $NiBr_2 \cdot 3H_2O$ with 2-hydroxymethylpyridine as the second example of cubane-type clusters with 2-hydroxymethylpyridine containing coordinate bromide. It is a new addition to cubane Ni_4^{II} clusters with an $S = 4$ ground state. In **1**, the asymmetric unit contains two independent $[Ni(hmp)(MeOH)Br]_4$ complexes, and each octahedral Ni(II) is bridged by four μ_3-CH_2O^- fragments from four hmp$^-$ ligands. The magnetic behavior for **1** indicates intracluster ferromagnetic coupling interactions stronger than $[Ni_4(Pym)_4Cl_4(CH_3OH)_4]$. The magnetoanisotropy value is $D = -0.65\,\text{cm}^{-1}$ and the best fit parameters are $J_1 = 8.56$, $J_2 = 2.28$, and $g \approx 2.13$.

Supplementary material

CCDC 772433 contains the supplementary crystallographic data of **1** for this article. These data can be obtained free of charge from the Cambridge Crystallographic Data Centre *via* www.ccdc.cam.ac.uk/data_request/cif.

Acknowledgments

This study was supported by the National Basic Research Program of China (2007CB925102), National Natural Science Foundation of China (NSFC: 20771056), State Basic Research Project of China (NSFC: 20490218), and the Center of Analysis and Determining of Nanjing University.

References

[1] P. Tola, O. Kahn, C. Chauvel, H. Coudanne. *New J. Chem. (Nouveau Journal De Chimie)*, **1**, 467 (1977).
[2] A. Caneschi, D. Gatteschi, R. Sessoli, A.L. Barra, L.C. Brunel, M. Guillot. *J. Am. Chem. Soc.*, **113**, 5873 (1991).
[3] R. Sessoli, H.L. Tsai, A.R. Schake, S.Y. Wang, J.B. Vincent, K. Folting, D. Gatteschi, G. Christou, D.N. Hendrickson. *J. Am. Chem. Soc.*, **115**, 1804 (1993).
[4] R. Sessoli, D. Gatteschi, A. Caneschi, M.A. Novak. *Nature*, **365**, 141 (1993).
[5] J.R. Friedman, M.P. Sarachik, J. Tejada, J. Maciejewski, R. Ziolo. *J. Appl. Phys.*, **79**, 6031 (1996).
[6] L. Thomas, F. Lionti, R. Ballou, D. Gatteschi, R. Sessoli, B. Barbara. *Nature*, **383**, 145 (1996).
[7] E.-C. Yang, W. Wernsdorfer, L.N. Zakharov, Y. Karaki, A. Yamaguchi, R.M. Isidro, G.D. Lu, S.A. Wilson, A.L. Rheingold, H. Ishimoto, D.N. Hendrickson. *Inorg. Chem.*, **45**, 529 (2006).
[8] J. Krzystek, J.H. Park, M.W. Meisel, M.A. Hitchman, H. Stratemeier, L.C. Brunel, J. Telser. *Inorg. Chem.*, **41**, 4478 (2002).
[9] G. Rogez, J.N. Rebilly, A.L. Barra, L. Sorace, G. Blondin, N. Kirchner, M. Duran, J. Van Slageren, S. Parsons, L. Ricard, A. Marvilliers, T. Mallah. *Angew. Chem. Int. Ed.*, **44**, 1876 (2005).
[10] R.E.P. Winpenny. *Adv. Inorg. Chem.*, **52**, 1 (2001).
[11] G.S. Papaefstathiou, S.P. Perlepes. *Comments Inorg. Chem.*, **23**, 249 (2002).
[12] M.L. Tong, S.L. Zheng, J.X. Shi, Y.X. Tong, H.K. Lee, X.M. Chen. *J. Chem. Soc., Dalton Trans*, 1727 (2002).
[13] A.J. Blake, C.M. Grant, S. Parsons, J.M. Rawson, R.E.P. Winpenny. *J. Chem. Soc., Chem. Commun*, 2363 (1994).
[14] S.T. Ochsenbein, M. Murrie, E. Rusanov, H. Stoeckli-Evans, C. Sekine, H.U. Güdel. *Inorg. Chem.*, **41**, 5133 (2002).
[15] A.L. Dearden, S. Parsons, R.E.P. Winpenny. *Angew. Chem. Int. Ed.*, **40**, 151 (2001).
[16] J. Ribas, A. Escuer, M. Monfort, R. Vicente, R. Cortes, L. Lezama, T. Rojo. *Coord. Chem. Rev.*, **193–195**, 1027 (1999).
[17] P.D.W. Boyd, R.L. Martin, G. Schwarzenbach. *Aust. J. Chem.*, **41**, 1449 (1988).
[18] M.A. Halcrow, J.S. Sun, J.C. Huffman, G. Christou. *Inorg. Chem.*, **34**, 4167 (1995).
[19] G. Aromi, A.S. Batsanov, P. Christian, M. Helliwell, O. Roubeau, G.A. Timco, R.E.P. Winpenny. *J. Chem. Soc., Dalton Trans*, 4466 (2003).
[20] M. Moragues-Canovas, M. Helliwell, L. Ricard, E. Riviere, W. Wernsdorfer, E.K. Brechin, T. Mallah. *Eur. J. Inorg. Chem*, 2219 (2004).
[21] J.E. Wertz, J.R. Bolton. *Electron Spin Resonance: Elementary Theory and Practical Applications*, Chapman & Hall, New York (1986).
[22] Siemens AXI Inc. *Software Packages SMART and SAINT*, Siemens Analytical X-ray Instrument Inc., Madison, WI (1996).

[23] G.M. Sheldrick. *SHELXL-97, Program for the Refinement of Crystal Structure*, University of Göttingen, Germany (1997).

[24] J.A. Mydosh. *Spin Glasses: An Experimental Introduction*, Taylor & Francis, London (1993).

[25] A. Escuer, M. Font-Bardia, S.B. Kumar, X. Solans, R. Vicente. *Polyhedron*, **18**, 909 (1999).

[26] M.P. Shores, J.J. Sokol, J.R. Long. *J. Am. Chem. Soc.*, **124**, 2279 (2002).

[27] J. Lawrence, E.-C. Yang, R. Edwards, M.M. Olmstead, C. Ramsey, N.S. Dalal, P.K. Gantzel, S. Hill, D.N. Hendrickson. *Inorg. Chem.*, **47**, 1965 (2008).